A Neural Network Model for Chemotaxis in Caenorhabditis elegans

N.A. Dunn[1], J. S. Conery[2], S.R. Lockery[1]*

1. Inst. of Neuroscience, 2. Dept. Computer Science

University of Oregon, Eugene OR 97403

***Abstract*-In *Caenorhabditis elegans*, spatial orientation behavior in a chemical gradient (chemotaxis) involves bouts of turning (pirouettes) modulated by the change in concentration of attractant. Ablation of identified neurons has delineated a candidate neural network for chemotaxis in *C. elegans*. The aim of our research is to generate testable models of how the network computes behavioral state and consequently, turning frequency, in response to changes in concentration.**

We were able to train neural networks to exhibit known chemotaxis rules using experimental data from chemotaxing *C. elegans*. The resultant network solutions involved three to five dynamically contributing neurons. Here we have analyzed the three neuron solutions and found three distinguishing features: a fast excitatory and delayed inhibitory connection, which acts as a differentiator; self-connections, which act to regulate neural response speed similar to synaptic time-constants; and recurrent inhibitory connections, which regulate second order network response characteristics. We plan to use this model to predict and interpret the results of laser ablations of neurons and genetic mutation in the *C. elegans* chemotaxis network.

I. Introduction

C. elegans is a relatively simple organism, consisting of 302 neurons and approximately 5600 synapses [1]. Their entire genome has also been sequenced. The combination of a simple chemotaxis behavior (movement in response to a chemical gradient), fully documented genetics, and a relatively simple neural connectivity pattern, makes *C. elegans* desirable as a model in which to study the neural network basis for chemotaxis computation.

Previous neural network studies in *C. elegans* chemotaxis have focused on neuronal ablations and genetic mutation. Ablation studies have primarily concentrated on overall functional degradation using lesion analysis [2]. While this work is essential for determining which neurons are responsible for chemotaxis, it cannot be used to determine the function of individual connections, such as connection strength or whether connections are excitatory or inhibitory.

C. elegans uses a combination of forward swimming and random turns during chemotaxis towards an attractant [3]. Behavior is modulated by the time rate of change in concentration, implying that the neural network responsible for chemotaxis differentiates concentration input over time. In this analysis, we use concentration data from chemotaxing *C. elegans*, which embodies this rule, to train model neural networks. The networks created should suggest neural network architectures for performing differentiation, yielding models that are testable by neuronal ablation and genetic mutation.

To train the model network, training data must represent the pirouette hypothesis for chemotaxis in *C. elegans*. The observed rule is that *C. elegans* is more likely to engage in a bout of one or more random sharp-turns, defined as pirouettes, when the concentration change of a moving worm decreases beyond an experimentally determined threshold [3]. When concentration increases, however, random sharp-turns turns are suppressed. This behavioral model loosely follows the chemotaxis algorithms observed in other organisms, e.g., E. coli [4], where dips in concentration increase the likelihood of random orientation behavior. This approach to network modeling and training was taken due to the stochastic nature of the experimentally observed rules. The stochastic behavior of the *C. elegans* makes it difficult to relate specific input back to a set deterministic behavior a neural network might produce.

Following training, networks were analyzed to determine connection architectures which produce the chemotaxis behavior observed in C. elegans. To validate our methodology, we simulated chemotaxis in a Petri dish using the trained neural networks.

II. Methods

A. Training Data

To produce network training stimulus, we used concentration data from a worm chemotaxing in a gradient of attractant. Training targets have one of three possible behavioral states at any one time: run, rest, or pirouette. Pirouette behavior has a higher sharp-turn movement probability, which correlates to a worm which sees a drop in concentration. Run behavior yields a higher forward swim movement probability, which correlates to a worm which sees an increase in concentration, suppressing random sharp-turns. Rest behavior represents a control, where the worm is

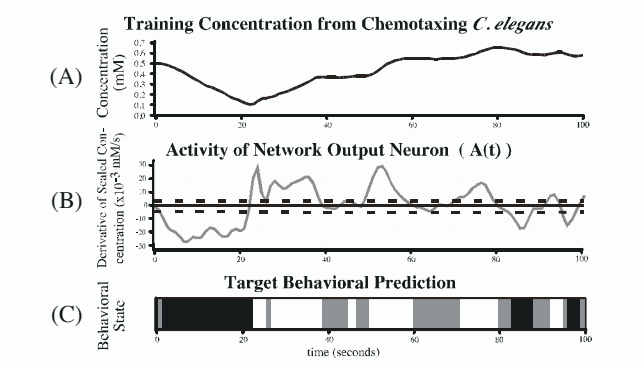

Fig. 1. Creation of training data. (A) The training target is constructed concentration data recorded from C. elegans chemotaxing towards an attractant at the center of a radial gradient. (B) The concentration track is differentiated and a threshold (dotted lines represent the upper and lower limits) is applied to yield a behavior. (C) White, where dC/dt>>0, represents run; grey, where dC/dt≈0, represents rest; and black, where dC/dt<<0, represents pirouette.

exposed to no chemical gradient.

The targets were created, as shown in Fig. 1, by looking at the instantaneous change of the stimulus concentration and applying the experimentally observed threshold, which yields one of the three behavioral states. These probabilities correlate to the likelihood of performing forward swim movement or random sharp-turns.

B. Network Model

We created a model neural network based on the neural network in *C. elegans* believed to be responsible for chemotaxis towards the attractant NH_4Cl (as well as other attractants) [5]. This candidate biological network contains 11 pairs of neurons. These neurons are shown in Fig. 2., where symmetric pairs are represented as single neurons. This neural network contains the chemosensory neuron pair ASE [5], eight inter-neuron pairs, and two command neuron clusters, AVA and AVB, which regulate forward versus pirouette behavior [6].

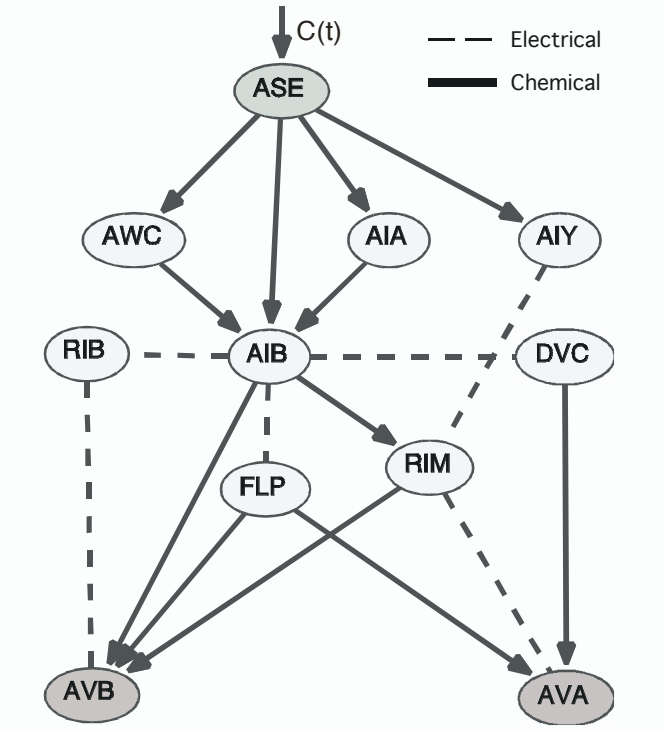

Fig. 2. A candidate chemotaxis network. Neuron pairs are represented as single neurons. The AVA command interneurons are believed to be responsible for turning behavior, while AVB is thought to be needed for forward movement [6].

Similar to the biological model, our network model, shown in Fig. 3, contains 10 neurons. The ASE pair is modeled as the only chemosensory input, since only ASER only responsds NH_4Cl (in this case the Cl^- ion) [5]. The eight interneurons pairs identified in the *C. elegans* chemotaxis network are derived from known connectivity pathways [1]. They are modeled as eight recurrent interneurons with self-connections, which connect to every neuron in the network,

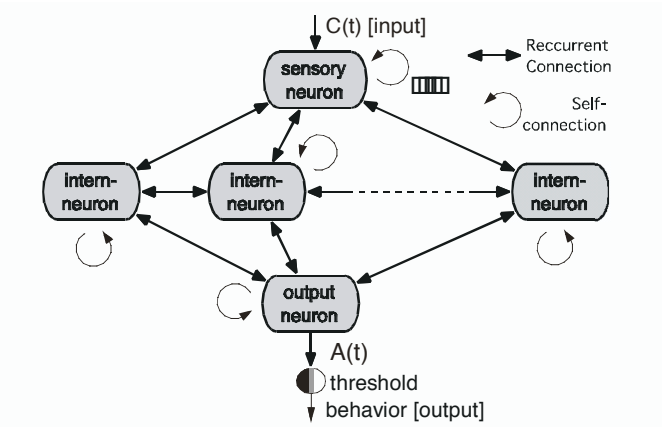

Fig. 3. The network model representing the candidate neural networks. The model has one chemosensory input, one command-neuron output, and eight fully-connected interneurons. The activity of the output neuron has a threshold applied to it, producing one of three behaviors: run, pirouette, or rest.

including the input and output neuron. Worm behavior is regulated by a single output neuron, an abstraction of the two command neuron pools. A high and low threshold is placed on the output neuron to partition the different behavioral states in *C. elegans*: run, pirouette, and rest.

$$\tau_i \frac{dA_i(t)}{dt} = \sigma_i(t) - A_i(t) \quad (1)$$

$$\sigma_i(t) = \frac{1}{1 + \exp\left[-\left(\sum (wt_i A_i(t)) - bias_i + stim(t)\right)\right]} \quad (2)$$

To allow our model to converge upon a range of good solution, neurons are modeled as fully-recurrent with self-connections. Neuronal activity is modeled as a sigmoid, as shown in (1) and (2). Stimulus input is fed to the input neuron, only. To reduce training time, the best threshold limits on the output neuron are deduced by linearly adjusting the upper and lower limits for a given network and training data set.

C. Training

Networks were trained using simulated annealing over a distributed architecture. Our annealing algorithm was written in C++ using MPI. The training algorithm was run over a Linux cluster consisting of 11 1-GHz Athlon processors running the Slackware Linux distribution.

Valid networks were selected based on a conservative error threshold. The threshold was determined qualitatively, comparing targets to trained network outputs with known error. The error threshold was chosen to make sure that the networks would not miss large behavioral predictions. Penalty per time-step was assessed as twice as much when the network mistakes run behavior for pirouette behavior (or vice versa). This is in contrast to the lesser mistake of predicting run or pirouette behavior instead of rest behavior.

Networks were pruned after training in order to analyze the minimal set of functional neurons. Pruning was performed

by clamping neurons, one at a time, to their average value (when experiencing the training stimulus) and determining if the change in error was greater than the error threshold allowed. At the end of the clamping cycle, all inactive neurons were discarded while their average neuronal values were distributed to downstream neurons as bias.

D. Simulation Model

To test whether our model was capable of producing biological chemotaxis behavior, we simulated worms chemotaxing within a chemical gradient using our trained neural networks to control chemotaxis behavior. The stimulus for each worm, and its associated chemotaxis neural network, is the attractant concentration at the point the worm sees on the dish at each time-step. As in training, the continuous stimulus into the network yields a continuous output on the decision making output neuron. This output has a threshold applied to it, which yields one of the three behavioral probability states: run, rest, or pirouette.

The simulation environment consisted of a worm being placed on a 9 cm Petri dish with a Gaussian distribution of attractant. Attractant concentration was greatest at the center of the dish. The worms were allowed two types of movement based on their behavioral state, random sharp turn (>50 degrees) or forward movement (<5 degrees, either way) [3]. The speed of forward movement is 0.15 mm/s, and sharp-turn speed is 0.1 mm/s [3]. From experimental data, where a pirouette is a bout of one or more sharp-turns, forward behavior has a sharp-turn probability of 0%, rest has a sharp-turn probability of 8%, and pirouette has a sharp-turn probability of 33% [7]. Thresholds of the model networks were set to those yielding the best fit during training.

III. Results

A. Training and Reduction

After the model networks had been trained, we confirmed their viability through generalization. Trained networks were given both the inverse (vertically flipped around average) of the training data as well as concentration data from another

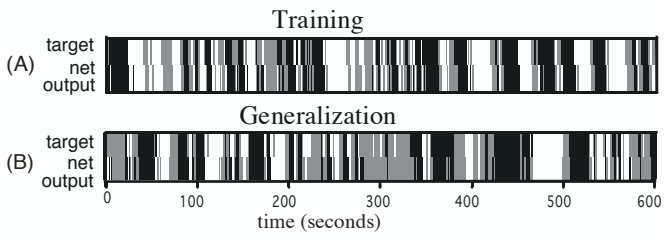

Fig. 4. A trained network generalized onto another worm track. White is run behavior, grey is rest behavior, and black is pirouette behavior. The top row in each figure is the target, generated from concentration data with a threshold applied to it from a *C. elegans* chemotaxing in a radial gradient (as in Fig. 1). The bottom row in each figure is the network output created from the same concentration input as the target. (A) Target data is from the same set as that which the neural network was trained. (B) Target data from a worm not used during neural network training.

chemotaxing worm as stimulus. As seen in Fig. 4., data from other worms' chemotaxis tracks yielded similar results,

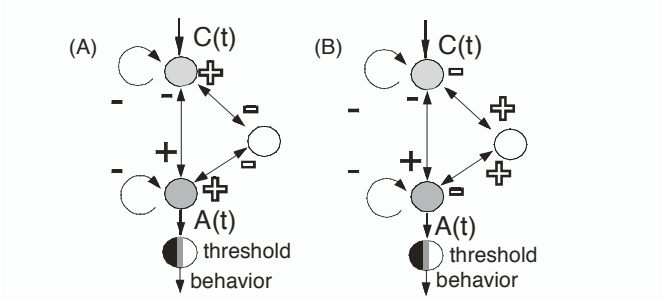

Fig. 5. Two network patterns exhibited in the three neuron networks. The outlined signs indicate differences between the two networks. (+) represents excitatory connections while (-) represents inhibitory connections.

allowing for only minor discrepancies in behavioral predictions.

After training, the networks were pruned in order to isolate the important network architectures This gave us a dispersion of three to five neuron networks, 100 of which were three neuron solutions. 58 of the 100 three neuron solutions were trained with no target delay. We believe that the four and five neuron networks emulate the architecture of the three neuron networks with redundant functionality, but this has yet to be determined.

B. Network Patterns

After training and pruning, three neuron networks were analyzed to determine common network components. Two network patterns emerged when analyzing three neuron networks for common behavioral patterns. Fig. 5. shows that the direct connection from the input to the output neuron is preserved in both networks, as well as the self-connection on each neuron. The difference between the two networks is the path from the input neuron to the output neuron via the inter-neuron.

The two networks shown in Fig. 5 can be simplified to a single pattern. The product of the signs going from the input neuron to the output neuron, through the interneuron, has a net inhibitory effect in both patterns (where the product of an inhibitory and excitatory connection is inhibitory). Additionally, the product of the connection loop between any two neurons has an inhibitory product. Therefore, the path through the interneuron represents the same pattern in both networks, since each forward connection retains a recurrent inhibitory loop. This results in a single pattern containing the three network features shown in Table 1: fast

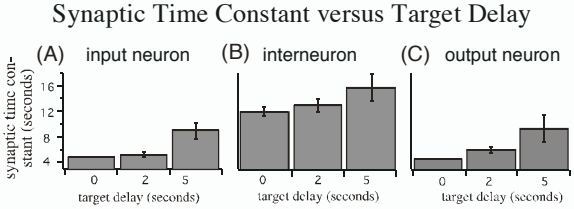

Fig. 6. Synaptic time constant from trained networks pruned to three neurons. The synaptic time constant becomes larger with increasing target delay. The synaptic time constant is consistently larger on the interneuron (B) than on the input (A) or output neuron (C).

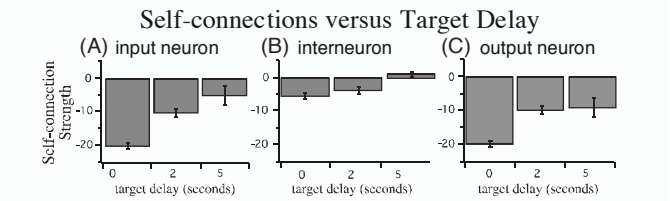

Fig. 7. Self-connections from trained networks pruned to three neurons. Self-connections become more positive with increasing target delay, indicating a quicker neuronal response which is inversely proportional to the synaptic time constant. Self-connections are more positive on the interneuron (B) than on the input (A) and output (C) connections, indicating that the interneuron is delayed.

excitatory/slow inhibitory parallel forward connections; inhibitory self-connections; and inhibitory recurrent loops.

C. *Network Component Analysis*

To determine the functionality of the three common components in our trained network, we looked at network patterns occurring between neurons and networks trained with varying

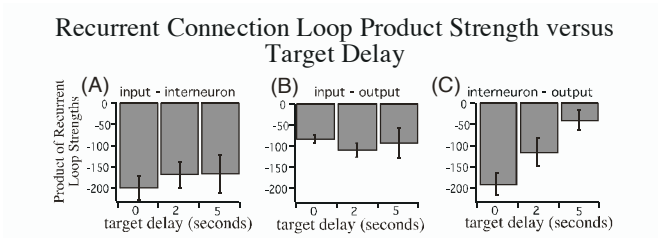

Fig. 8. The product of weights for recurrent inhibitory loops from trained networks pruned to three neurons. Every recurrent loop product is negative (i.e., has one excitatory and one inhibitory connection). Only the interneuron to output neuron loop (C) responds to increasing target delay.

amounts of delay between the training stimulus and target. By training with an increasing delay between the target and the stimulus, we should be able to see what features regulate network response, and how the different network features interact. In this case, we looked at synaptic time constants, self-connections, and inhibitory recurrent loops.

From Fig. 6, we can see that synaptic time constants increase as the delay between the stimulus and the target becomes greater. The synaptic time constant is directly proportional to the target delay. As we see in Fig's. 6 and 7, the size of the inhibitory self-connections are inversely proportional to the target delay. Both the small synaptic time-constants and large inhibitory self-connections increase the speed of neuronal response.

TABLE I
Dominant features of trained three neuron model networks.

Feature	Figure	Function
direct excitatory delayed inhibitory	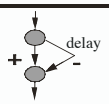	differentiation
self-connection		increases speed of neural response
recurrent inhibitory loop		modulates dampening of neural response

The interneurons shown in Fig's. 6 and 7 have larger synaptic time constants and smaller self-connections than the input and output neurons. This indicates a delay in the interneuron. The delayed inhibitory forward connection, going through the interneuron, and the fast excitatory connection, going directly from the input to the output neuron, form a classic differentiator (shown in Table 1).

Inhibitory recurrent loops have a less obvious role in the network. Fig. 8. shows that every forward connection has a corresponding recurrent inhibitory connections, forming a recurrent loop. Altering the target delay only affects the relative strength of one of the recurrent loops, the output neuron to interneuron loop. Increased target delay reduces the magnitude of this loop. This suggests that the reduced connection strength of the recurrent loop reduces the speed of the network response to a stimulus.

We observed patterns from 58 randomly trained networks which had been pruned to three neurons. We were able to identify the three common features of these networks, shown in Table 1. 42 three neuron networks were trained with a delayed target, allowing us to further verify the function of these network features.

D. *Simulation Results*

To validate our approach, we simulated *C. elegans* chemotaxing using a trained network. Fig. 9 compares the chemotaxis tracks of an experimentally observed animal (A) to those of a simulated worm using a trained, model neural network to guide chemotaxis (B). In both cases, the worms make it to the attractant center and stays there using a series of random sharp-turns and forward swimming movements.

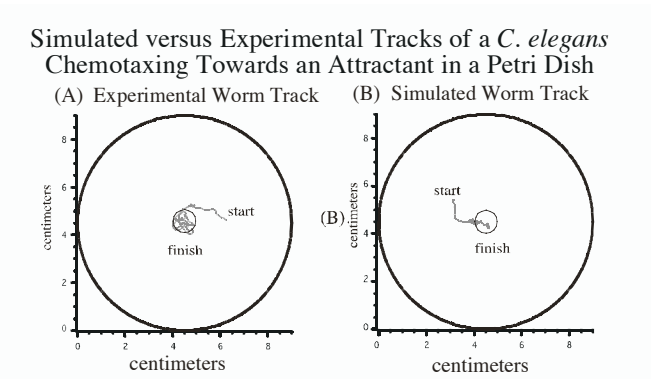

Fig. 9. (A) A sample track of a live C. elegans chemotaxing and (B) a simulation of a chemotaxing C. elegans using a fully-trained network. Both tracks represent radial gradients of attractant with highest concentration at the center. Successful chemotaxis is defined as reaching within a 0.5 cm radius from the center. Average starting position is within 1.1 cm from the center.

We compared several experimental and simulated results, and got similar probabilities for success, suggesting that our trained model neural networks are able to simulate the network responsible for chemotaxis behavior observed in *C. elegans*.

IV: Conclusion

In this analysis, we created a model neural network for chemotaxis in *C. elegans* based on an experimentally observed rule, our goal being to guide future neuronal ablation and genetic mutation studies. This rule computes the change in concentration and applies a threshold to that value, which is used to turning behavior.

To create the model network, we trained a model 10 neuron neural network, based on the biological chemotaxis network, to implement an experimentally observed rule for chemotaxis. The trained neural networks were then pruned, resulting in three to five neuron networks. Upon analyzing the three neuron networks, we were able to arrive at a single network pattern. The three neuron networks had three dominant features (Table 1): a fast excitatory pathway in parallel with a delayed inhibitory pathway, inhibitory self-connections, and recurrent, inhibitory, two neuron loops. Furthermore, we were able to simulate *C. elegans* chemotaxing towards an attractant in a radial gradient by using these trained networks to produce behavioral states.

From the trained network patterns, we predicted plausible patterns of connectivity in the *C. elegans* chemotaxis network. The fast excitatory/slow inhibitory network forms a classic differentiator pattern. It was unsurprising that our networks would create a neural network capable of differentiating, given our training rule. However, it was surprising that all the networks exhibited the common features shown in Table 1, since network connectivity patterns were quite varied. The two other network features, the negative recurrent loops and the self-connection, can be seen as supporting features to the differentiator backbone.

Future work in the live animal is needed in order to determine if these features exist as shown. In the biological implementation, the differentiator can be expressed as shown in Fig. 5, or as simply as a gap-junction coupled with a slower inhibitory chemical synapse. Additionally, self-connections may represent symmetrical pairs of neurons which connect to each other. Recurrent inhibitory connections may exist in numerous places in *C. elegans*, since many interneurons are connected both ways.

A shortfall of this model is that the experimental conditions given to *C. elegans* to generate our experimental rule were generated in an environment where the worm receives constant dynamic input. This is because the concentration is constantly changing as the worm moves up and down a gradient in the Petri dish. The resultant long-term response is a convolution of responses to several chemotaxis stimuli, instead of a well-correlated stimulus and response. This still gives accurate short-term responses to concentration stimuli, which have been validated via step and pulse-responses. However, these step and impulse tests in the live animal, have also shown that long-term responses may not have been accounted for in this model.

To diminish the affects of convolution of responses from nonlinear stimuli, further modeling will concentrate on step and pulse stimulus data. We would also like to extend our model to take into account the two neural pools in *C. elegans* believed to be key for forward and turning behavior, AVA and AVB [6]. Our current model abstracts these connections into a single neuron output. This analysis may also look at the dynamic interaction between AVA and AVB in order to explain the stochastic nature of the behavior exhibited.

This modeling methodology can also be applied to other sensory stimuli in *C. elegans*, including thermotaxis and mechanosensory, which are believed to implement the same forward and turning neuron cluster [6][8], but through differing interneuronal pathways.

Acknowledgment

I would like to thank the members of the Lockery Lab for many valuable discussions and Don Pate for his invaluable hardware expertise.

References

[1] J.G. White,, E. Southgate, J.N. Thompson, S. Brenner, *The Structure of the nervous system of the nematode* Caenorhabditis elegans. Philos Trans R Soc Lond, vol 314, pp. 1-340, 1986

[2] C.I. Bargmann, E. Hartwieg, H. R. Horvitz, "Odorant-selective genes and neurons mediate olfaction in *C. elegans*." *Cell*, vol. 74, pp. 515-527, 1993

[3] J.T. Pierce-Shimomura, T.M. Morse, & S.R. Lockery, "The fundamental role of pirouettes in *Caenorhabditis elegans* chemotaxis." *J. Neuroscience*, vol. 19, pp. 9557-9569, 1999

[4] S.M. Block, J.E. Segall, H.C. Berg, "Impulse responses in bacterial chemotaxis." *Cell*, vol. 31, pp. 516-226, 1982

[5] C.I. Bargmann, H. R. Horvitz, "Chemosensory neurons with overlapping functions direct chemotaxis to multiple chemicals in *C. elegans*." *Neuron*, vol. 7, pp. 729-742, 1991

[6] S.R. Wicks, C.J. Roehrig, C.H. Rankin, "A dynamic network simulation of the nematode tap withdrawal circuit: predictions concerning synaptic function using behavioral criteria." *The Journal of Neuroscience*, vol. 16, pp. 4017-4031

[7] S.R. Lockery, unpublished

[8] I. Mori, Y. Ohshima, "Neural regulation of thermotaxis in *Caenorhabditis elegans*." *Nature*, vol. 376, pp. 344-348, 1995